



## EFFECT OF ROCKING FOUNDATION INPUT MOTION ON THE NONLINEAR RESPONSE CHARACTERISTICS OF SUPERSTRUCTURE

O.C. Ogut<sup>(1)</sup>, M. Mori<sup>(2)</sup>, N. Fukuwa<sup>(3)</sup>

<sup>(1)</sup> Grad. Student, Graduate School of Environmental. Studies, Nagoya University, ogut@sharaku.nuac.nagoya-u.ac.jp

<sup>(2)</sup> Designated Prof., Disaster Mitigation Research Center, Nagoya University, Dr. Eng., m.mori@sharaku.nuac.nagoya-u.ac.jp

<sup>(3)</sup> Prof., Disaster Mitigation Research Center, Nagoya University, Dr. Eng., fukuwa@sharaku.nuac.nagoya-u.ac.jp

...

### **Abstract**

In this study, it is tried to determine the response characteristics of the superstructures according to embedment depth and mechanical properties of the superstructure. A new lumped parameter model (LPM) is constructed depend on the impedances of embedded foundations having different embedment depth placed on the elastic half-space modeled by thin layers for the Poisson Ratio value equals to 0.42 and shear wave velocity value equals to 100 and 200 m/s to represent the soft soil conditions. After that non-linear earthquake response analyses by using the proposed LPM model are carried out considering with and without rocking foundation input motion (RFIM) to get effects of RFIM on the ductility demands of structures. Analyses are done for different embedment ratios ( $e/r$ ) which equal to 0, 0.5, 1.0, and 2.0.

It is concluded about the embedment depth that when ductility capacities under the fixed based condition ( $\mu_{fix}$ ) is small, the responses of buildings with natural periods more than 2 seconds except for the  $e/r = 2$  under considering the rocking foundation input motion are smaller than those of the fixed-base model. It is estimated that the input ground motion is reduced because the slender building with spread foundation on soft ground is assumed and the rocking spring of the soil is relatively small and the natural period of the coupled system becomes long. However, if the embedment is deep ( $e/r = 2.0$ ) considering the rocking input motion, it is seen that the response is increasing because of the small rocking stiffness. By increasing ductility factor values, the effect of RFIM becomes more important especially for high-rise buildings having deep embedment ratios. The reason of this phenomenon is considered that equivalent elastic stiffness of superstructure becomes softer for increasing values of ductility capacity, therefore inertial interaction becomes less important and the additional force coming from the rocking motion becomes more important on the response of superstructure. Therefore, RFIM should be considered for the collapse limiting design especially for the high rise building having deep embedded foundations for this case.

*Keywords: Soil-structure interaction; Nonlinear structural analysis; Lumped parameter models; Foundation input motion*



## 1. Introduction

This is prepared for the presentation of an academic paper [1]. For determining the damage to structures during strong earthquakes, soil-structure interaction (SSI) becomes very important in some situations especially for low and middle rise buildings. Therefore, researches on this topic are necessary for reliable earthquake resistance design to understand the key parameters of SSI that influence on inelastic behavior of superstructures.

As it is known, the SSI effect can be analyzed under the subtopics named as kinematic interaction (KI) which occurs due to rigidity differences of foundations and the surrounding soil, and inertial interaction which relates to mass properties of the structure. In the pioneering works [2-5], a replacement oscillator is improved, which has modified period and damping values according to SSI effect for the single degree of freedom system (SDOF) by taking the foundation input motion (FIM) as free field motion (FFM) because of surface foundation situation. Although their approximation is reasonable only for surface foundations, Bielak [6], and Aviles and Perez-Rocha [7] analyze the response of embedded foundations under the FFM neglecting the effect of KI. KI is also neglected at some American design codes [8-10]. On the other hand, in FEMA 440 [11], FEMA P-1050 [12] and Japanese design code [13], KI is considered but rocking foundation input motion (RFIM) is not considered. Nevertheless, according to Luco [14], using the horizontal foundation input motion (HFIM) and RFIM instead of FFM is important for reasonable designs. Moreover, according to Morray [15], the peak values of the acceleration response spectra are underestimated if the effect of the RFIM is neglected. Therefore, the sensitivity of analyses on RFIM should be researched.

All the aforementioned studies include only elastic soil-structure systems. However, as it is known, structures response beyond the elastic region of the material during strong earthquakes. The early study about the response of elasto-plastic structure considering SSI is done by Veletsos and Vebric [16]. In their study, it is asserted that the effect of inelasticity of structure diminishes the relative stiffness of structure to the soil, therefore the effect of SSI decreases the response. According to Bielak [17], on the resonant frequency, structural deformations become large for an inelastic structure having a surface foundation. Lin and Miranda [18] research the effect of SSI on the maximum inelastic deformation of SDOF systems by taking the KI effect as the low-pass filter. Jarenpasert *et al.* [19] analyze the SDOF elasto-plastic structure embedded in elastic soil without the KI effect. Pitilakis and Makris [20] conduct dimensionless analysis to determine seismic demand of yielding structures interacting with soil and it is asserted that seismic demand increase with increasing foundation soil mass and yielding displacement and SSI is not always beneficial for inelastic responses of superstructures. Karatzetzou and Pitilakis [21] criticize the reliability of FEMA 440 [11] design code for determining performance-based seismic demand and it is claimed that FEMA 440 [11] gives unreliable results for such analyses. Moreover, Mahsuli and Ghannad [22] assert that ductility demands for embedded foundations increase with increasing their embedment ratios, especially for the embedment ratios bigger than one due to the effect of RFIM. And in their study the lumped parameter model (LPM) given as Wolf [23] for embedded foundations is used as a soil model for the analyses. Although this model is very convenient to consider the nonlinearity of superstructures due to having frequency independent elements, it is improved for Poisson's ratio of soil ( $\nu$ ) equals to 0.25 because of the lack of reliable data for other values of  $\nu$ . However, as it is known, for soft soil conditions, where SSI effects can be seen more severely, Poisson's ratios are observed higher, up to 0.5. Moreover, in the aforementioned study, height of the SDOF structure is taken independently from the fixed base natural frequency which may represent unrealistic structural characteristics, and only records of active fault earthquakes are considered, so the results cannot be generalized to subduction zone related earthquakes.

In this study a new LPM is constructed depending on the impedances of embedded foundations having different embedment depths placed on the elastic half-space for the  $\nu$  equals to 0.42 and shear wave velocity value ( $V_s$ ) equal to 100 and 200 m/s to represent the soft soil conditions.  $\nu$  is selected as 0.42 as a case of soft soil condition and fixed for the analyses in this study. Moreover, it should be noted that this method is applicable for other  $\nu$  values. After that non-linear earthquake response analyses by using the proposed LPM model are carried out under active fault and subduction zone earthquake records considering with and without RFIM to get the effects of RFIM on the ductility demands of structures. Additionally, it can be said that the method of analysis is



more reliable than the Mahsuli and Ghannad [22], because the created LPM is more reliable for soft soil conditions ( $\nu$  equals to 0.42 instead of equal to 0.25) where SSI effect can be seen more severely and the parameters selected for the superstructure make easier to understand which kind of structures are affected from SSI intensively by taking predominant periods (between 0.2 and 3 seconds) of superstructures related to their aspect ratios and assuming the ductility capacities under the fixed based condition ( $\mu_{fix}$ ) as 2, 4, and 6.

## 2. Analysis Model and Method

### 2.1 Analysis method

As it is known, determining the exact impedances and input motions for foundations requires time consuming mathematical techniques such as the finite element method. To manage this, Meek and Wolf [24] assert a simplified method by using double cone analysis to obtain the impedances and FIM of embedded foundations. Due to the simplicity, in this study, the lumped parameter method improved by Wolf [23] is used and the horizontal and rocking foundation input motions are calculated by double cone analysis [25].

### 2.2 Outline of new LPM

In this study, a new LPM is improved by using the systematic procedure of Wolf [23] for the  $\nu$  equals to 0.42. In this method the exact values of dynamic stiffness, which are obtained by different techniques such as the thin layer method (TLM), are divided into the regular and singular part (the value of the impedance calculated by using dimensionless spring and dashpot values for infinite frequency) as it is seen in Eq. (1), (2) and (3) respectively according to the rule of Wolf [23]. In these equations  $S$  is the dynamic stiffness,  $S_s$  is the singular part of the dynamic stiffness,  $S_r$  is the remaining regular part of the dynamic stiffness,  $K$  is the static stiffness,  $p$  and  $q$  are real coefficients of the polynomials,  $N$  is the degree of polynomial placed on the denominator,  $k(a_0)$  and  $c(a_0)$  are spring and dashpot coefficients of the dynamic stiffness,  $k$  and  $c$  are values of spring and dashpot coefficients of the dynamic stiffness at the infinite frequency, and  $a_0$  is the dimensionless frequency that is given in Eq. (4), where  $\omega$  is the circular frequency, and  $r$  is the radius of the foundation.

$$S(a_0) = K[k(a_0) + ia_0c(a_0)] = S_s(a_0) + S_r(a_0) \quad (1)$$

$$\frac{S_s(a_0)}{K} = k + ia_0c \quad (2)$$

$$\frac{S_r(a_0)}{K} = \frac{S_r(ia_0)}{K} = \frac{P(ia_0)}{KQ(ia_0)} = \frac{1 - k + p_1ia_0 + p_2(ia_0)^2 + \dots + p_{N-1}(ia_0)^{N-1}}{1 + q_1ia_0 + q_2(ia_0)^2 + \dots + q_N(ia_0)^N} \quad (3)$$

$$a_0 = \frac{\omega r}{V_s} \quad (4)$$

Next,  $2N-1$  real unknown  $p_1, \dots, p_{N-1}$  and  $q_1, \dots, q_N$  are determined by curve fitting technique on  $S_r$  by using the least square method to obtain a minimum  $\varepsilon^2$  value as it is seen in Eq. (5) where  $Q$  and  $P$  represent the polynomials placed on the numerator and denominator of Eq. (3) respectively and  $w(a_0)$  is the weight function.

$$\varepsilon^2 = \sum_{j=1}^J w(a_{0j}) |S_r(a_{0j})Q(ia_{0j}) - P(ia_{0j})|^2 \quad (5)$$

After that, the regular part of the dynamic stiffness is written in the form of the partial fraction expansion at Eq. (6) where  $s_\ell$  are the roots of  $Q$ ,  $A_\ell$  are the residues at the poles.

Since the  $N$  is taken as 1 in this study, Eq. (6) can be written in the form of Eq. (7) for  $N=1$ .

$$\frac{S_r(ia_0)}{K} = \sum_{\ell=1}^N \frac{A_\ell}{ia_0 - s_\ell} \quad (6)$$

$$\frac{S_r(ia_0)}{K} = \frac{A_1}{ia_0 - s_1} \quad (7)$$

The dynamic stiffness of the foundation can be represented by a combination of the models seen in Fig.1(a) and (b) physically. If we consider the dynamic stiffness of the model seen in Fig.1(a) and given in Eq. (8), we can easily determine the  $A_1$  and  $s_1$  values to match the dynamic stiffness of the model to the regular part of the dynamic stiffness by using Eqs. (9)-(10). And the singular part of the dynamic stiffness can be represented by the model seen in Fig.1(a). This systematic lumped parameter method rule is taken from Wolf [23].

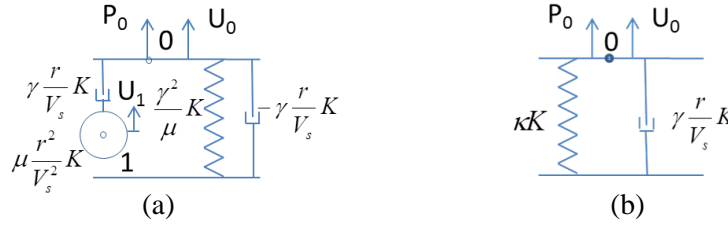


Fig. 1 – The model selected to the regular (a) and the singular part (b) of the dynamic stiffness

$$\left( \begin{array}{c} \frac{\gamma^3}{\mu^2} \\ ia_0 + \frac{\gamma}{\mu} \end{array} \right) U_0(a_0) = \frac{P_0(a_0)}{K} \quad (8)$$

$$\gamma = \frac{A}{s_1^2} \quad (9)$$

$$\mu = -\frac{A}{s_1^3} \quad (10)$$

The aforementioned technique is reliable when coupling is neglected. However, as it is known, horizontal and rocking degree of freedoms of embedded foundations interact with each other. To manage this, discrete impedance values represented by horizontal, rocking and coupling parts of the model are calculated as it is shown in Eqs. (11)-(13), where  $e$  is the embedment depth of the foundation,  $S_{hh}$ ,  $S_{rr}$ , and  $S_{hr}$  are horizontal, rocking, coupling dynamic stiffness values of the rigid foundation respectively.  $S_{hh}^m$ ,  $S_{rr}^m$ , and  $S_{hr}^m$  are dynamic stiffness values of horizontal, rocking, and coupling part of this model respectively. By using this discretization, the curve fitting technique can be applied to each part of the model separately.

The new model is shown in Fig.2. The main difference of this model from that introduced by Wolf [23] for embedded foundations is that this model has a fictitious mass not only for rocking part but also for coupling part due to the high frequency dependence of the coupling impedance.

The dynamic stiffness of horizontal, rocking and coupling part of the model seen in Fig.2 are given in Eqs. (14)-(16) respectively.

Equations of the parameters are given in Eqs. (17)-(22) where  $C_1$ ,  $C_2$ ,  $M_1$ ,  $M_2$  and  $K$  are lumped values for damping, mass and spring having subindices  $h$  for horizontal,  $r$  for rocking,  $hr$  for coupling component of the model.  $K_{correct}$  is the correcting coefficient used for better fit to exact impedances.  $K_{hh}^m$ ,  $K_{rr}^m$ ,  $K_{hr}^m$  represents the static stiffness of horizontal, rocking and coupling part of the model respectively.  $\gamma_1$ ,  $\gamma_2$ ,  $\mu_1$ , and  $\mu_2$  are dimensionless values.

$$S_{hr}^m(\omega) = -\frac{S_{hr}(\omega)}{e} \quad (11)$$

$$S_{hh}^m(\omega) = S_{hh}(\omega) + \frac{S_{hr}(\omega)}{e} \quad (12)$$

(13)

$$S_{rr}^m(\omega) = S_{rr}(\omega) + eS_{hr}(\omega)$$

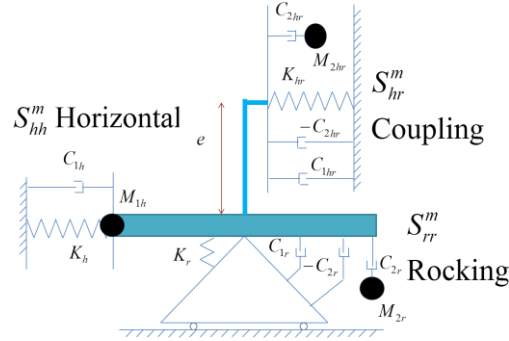


Fig. 2 – A new LPM model produced in this study

$$S_{hh}^m(\omega) = (-\omega^2 M_{1h} + K_h + i\omega C_{1h}) \quad (14)$$

$$S_{rr}^m(\omega) = -\omega^2 M_{2r} + K_r + i\omega C_{1r} - i\omega C_{2r} \frac{i\omega C_{2r}}{-\omega^2 M_{2r} + i\omega C_{2r}} \quad (15)$$

$$S_{hr}^m(\omega) = -\omega^2 M_{1hr} + K_{hr} + i\omega C_{1hr} - i\omega C_{2hr} \frac{i\omega C_{2hr}}{-\omega^2 M_{2hr} + i\omega C_{2hr}} \quad (16)$$

Finally, the dimensionless coefficients of the model for different embedment ratios ( $e/r$ ) are given in Table 1. As it is seen in the table, there is no coupling part for surface foundation ( $e/r=0$ ), and coupling part for the embedment ratio which equals to 0.25 has only one spring and dashpot. It means that the coupling impedance does not so depend on excitation frequency for low embedment ratios. The verification of this LPM model is given in Ogut *et al.* [1].

$$C_{1h} = \gamma_{1h} \frac{r}{V_s} K_{hh}^m \quad C_{1r} = \gamma_{1r} \frac{r}{V_s} K_{rr}^m \quad C_{1hr} = \gamma_{1hr} \frac{r}{V_s} K_{hr}^m \quad C_{2r} = \gamma_{2r} \frac{r}{V_s} K_{rr}^m \quad C_{2hr} = \gamma_{2hr} \frac{r}{V_s} K_{hr}^m \quad (17)$$

$$M_{1h} = \mu_{1h} \frac{r^2}{V_s^2} K_{hh}^m \quad M_{2r} = \mu_{2r} \frac{r^2}{V_s^2} K_{rr}^m \quad M_{2hr} = \mu_{2hr} \frac{r^2}{V_s^2} K_{hr}^m \quad (18)$$

$$K_h = Kh_{correct} K_{hh}^m \quad K_r = Kr_{correct} K_{rr}^m \quad K_{hr} = Khr_{correct} K_{hr}^m \quad (19)$$

$$K_{hh}^m = \frac{16Gr}{3(2-\nu)} \left(1 + \frac{e}{r}\right) \quad (20)$$

$$K_{rr}^m = \frac{8Gr^3}{3(1-\nu)} \left(1 + 2.3 \frac{e}{r} + 0.58 \left(\frac{e}{r}\right)^3\right) - \frac{8Gr^3}{3(2-\nu)} \left(\frac{e^2}{r^2} + \frac{e^3}{r^3}\right) \quad (21)$$

$$K_{hr}^m = \frac{8Gr}{3(2-\nu)} \left(1 + \frac{e}{r}\right) \quad (22)$$

### 2.3 Determining the parameters of LPM

In this study, the impedances obtained by TLM analyses are assumed as exact values, and a new LPM is created by using the curve fitting technique improved by Wolf [23] on these impedances. The soil and foundation model can be seen in Fig.3. To calculate the homogeneous elastic half-space by TLM, the soil is divided into the thin layers with increasing thickness from bottom to top. Moreover, to represent unbounded soil, paraxial boundary is applied to the bottom of model. Moreover, a circular rigid foundation placed on this half-space is also divided into the elements to calculate impedances by using finite element method (FEM), as it is seen in Fig.3 (Wen [26]).

Table 1 – The dimensionless parameters of LPM for Poisson’s ratio equals to 0.42

	$e/r=0.00$	$e/r=0.25$	$e/r=0.50$	$e/r=1.00$	$e/r=1.50$	$e/r=2.00$
$Kh_{correct}$	1.000	1.109	1.102	1.050	0.995	0.948
$Kr_{correct}$	1.000	0.886	0.858	0.895	0.898	0.878
$Khr_{correct}$	1.000	0.605	0.936	1.056	1.069	1.057
$\gamma_{1h}$	0.608	0.552	0.798	1.064	1.241	1.416
$\gamma_{1r}$	0.460	0.450	0.421	0.268	0.019	-0.355
$\gamma_{1hr}$	-	1.694	1.224	1.627	1.930	2.168
$\gamma_{2r}$	0.413	0.436	0.406	0.381	0.440	0.512
$\gamma_{2hr}$	-	-	0.082	0.416	0.514	0.575
$\mu_{1h}$	-	-	0.029	0.050	0.082	0.103
$\mu_{2r}$	0.178	0.190	0.165	0.145	0.194	0.263
$\mu_{2hr}$	-	-	0.007	0.173	0.264	0.330

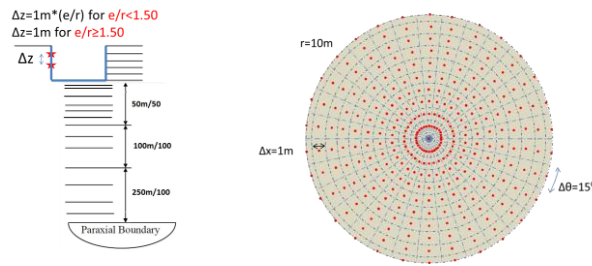


Fig. 3 – Soil model by TLM and model of the foundation by FEM

## 2.4 Determining driving forces

As it is known, driving forces are the forces required to make foundation motionless under the FIM. To get them, LPM should be analyzed in the frequency domain. Driving forces are given in Eq. (23), where  $P_g$  is horizontal driving force,  $M_g$  is rocking driving force,  $u_g$  is horizontal foundation input motion (HFIM) and  $\theta_g$  is RFIM.

$$\begin{bmatrix} S_{hh}(\omega) & S_{hr}(\omega) \\ S_{hr}(\omega) & S_{rr}(\omega) \end{bmatrix} \begin{Bmatrix} u_g(\omega) \\ \theta_g(\omega) \end{Bmatrix} = \begin{Bmatrix} P_g(\omega) \\ M_g(\omega) \end{Bmatrix} \quad (23)$$

If  $u_g$  and  $\theta_g$  are taken as given above, this situation equals to “with RFIM”. If  $\theta_g$  is taken as zero for same  $u_g$ , this situation equals to “without RFIM”. If  $u_g$  is taken as the free field motion (FFM) and  $\theta_g$  is taken as zero, this situation equals to “without KI” in this study. These situations are given in Fig.4 where  $u_f$  is FFM graphically. The differences of the effect of these situations on the nonlinear behavior of superstructure are researched.

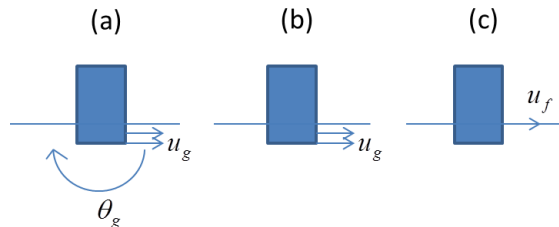


Fig. 4 – Analysis conditions (a) With RFIM, (b) Without RFIM, (c) Without KI

## 3. Analysis parameters

### 3.1 Model of SDOF structure

A simple approximation is applied to determine the parameters of the structure as it is seen in Fig.5(a), where  $T_{fix}$  is natural period of the SDOF system under the fixed base situation,  $N$  is the number of stories,  $M_{floor}$  is the mass

of each floor of the structure,  $b_{floor}$  is the thickness of the floor,  $b_{found}$  is the thickness of the foundation,  $\Delta H$  is the story height,  $H$  is the total height of the structure and  $H_{eff}$  is the effective height of the structure,  $m$  is the mass of superstructure and  $m_f$  is the mass of foundation. Mass ratio of the foundation to the structure ( $m_f/m$ ) is taken as 0.82 and analyses are done for the embedment ratios of foundations ( $e/r$ ) which equal to 0, 0.5, 1.0, and 2.0. Foundations are considered as infinitely rigid. The initial stiffness proportional damping is applied. Newmark-Beta Method is used and  $\beta$  is set as 0.25.

For simplicity, the inelasticity of structures is represented by elasto-plastic models with zero hardening after yielding as it seen in Fig.5(b). The yield strength is assumed so that the maximum ductility factor may equal to  $\mu_{fix}$  as a given value under the fixed base model.

### 3.2 Soil parameters

The soil is idealized as homogeneous elastic half-space having no material damping. Mass density of soil ( $\rho$ ) is considered as  $1.8 \text{ t/m}^3$ , and shear wave velocity of soil ( $V_s$ ) is selected as 100 and 200 m/s. To represent the soft soil condition, Poisson's ratio of soil ( $\nu$ ) is taken as 0.42.

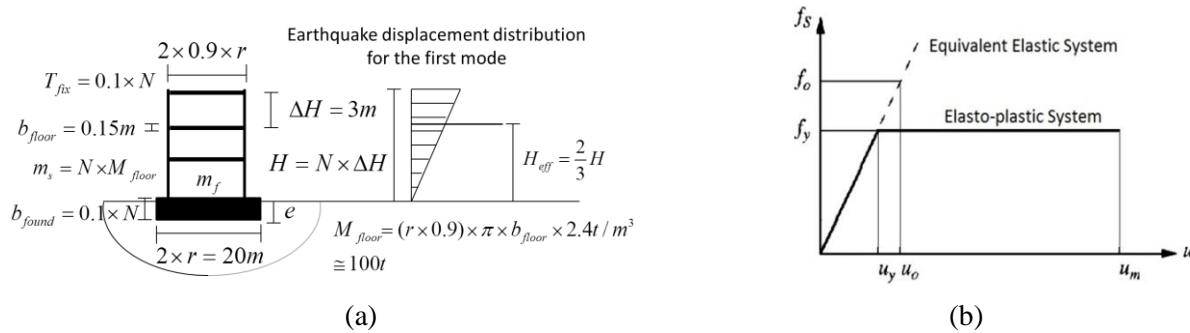


Fig. 5– (a) Analysis model for superstructures and (b) Elasto-plastic model of superstructures used in this study.  $f_0, f_y, u_0, u_y$  and  $u_m$  are the elastic demand of strength, yield strength, elastic displacement demand, yield displacement and ultimate displacement of the system, respectively

### 3.3 Selected Earthquake Records

The 1995 Hyogoken-Nanbu (Kobe Earthquake) TAK000 component of Takatori Station Record and the 2011 off the Pacific Coast of Tohoku Earthquake (Tohoku Earthquake) EW component of MYG006 Station (K-NET Furukawa) are chosen as input motions. The acceleration time histories and acceleration response spectra ( $h=5\%$ ) of the records are given in Fig.6.

## 4. Effect of RFIM on the non-linear response of superstructures

### 4.1 Analysis Results for Kobe Earthquake Record

In this section, non-linear seismic response analyses are applied using the proposed analytical model to determine the effect of the rocking foundation input motion (RFIM) on the responses of superstructures.

Time history non-linear response analyses are carried out under some input motions considering the KI by using the proposed analysis model. The effect of the RFIM on the non-linear response of the superstructure is studied by comparing the maximum ductility factor ( $\mu_{max}$ ) with  $\mu_{fix}$  in the case of the different embedment depth of foundation.

The results obtained by using Kobe Earthquake record are shown in Figs.7 – 8 where  $x$  axis is the natural period of the superstructure that represents number of stories of the superstructure from 2 to 30 stories. All figures show the ratio of  $\mu_{max}$  to  $\mu_{fix}$ . Figs.7 and 8(a-c) show the result for the shear wave velocity  $V_s = 100\text{m/s}$  of

soil model and  $\mu_{fix} = 2, 4, \text{ and } 6$ . Fig.8(d-f) shows the results in the case of the shear wave velocity  $V_s = 200\text{m/s}$  of soil model and  $\mu_{fix} = 2$ . In each figure, (a, d) with RFIM, (b, e) without RFIM, (c, f) without KI are given.

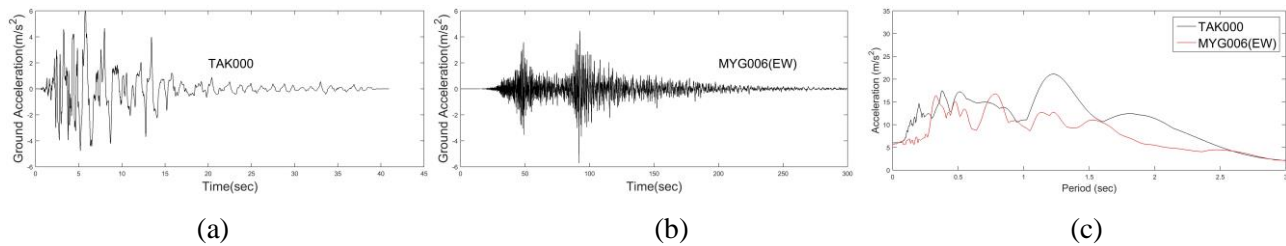


Fig. 6 – (a) Acceleration time history of Kobe Earthquake TAK000 component at Takatori Station, (b) Acceleration time history of Tohoku Earthquake EW component at MYG006 Station, and (c) Acceleration response spectra of TAK000, and MYG006 (EW) records ( $h=5\%$ )

First, the difference of the  $\mu_{max}$  values under the conditions (a) with RFIM and (c) without KI are expressed. As shown in Figs. 7 to 8 (a, d) and (c, f), it is observed that responses with RFIM are almost equal to those without KI for every  $\mu_{fix}$  of middle rise buildings, but responses of low rise buildings with short natural period (natural period less than 0.5 sec) for (a, d) are smaller than for (c, f) because of low-pass filter effect of KI. Therefore, it can be said that safer design is obtained for low rise buildings by neglecting KI.

Next, the difference of the  $\mu_{max}$  values under the conditions (a) with RFIM and (b) without RFIM are explained. It is clear that the responses of (b) are smaller than that of (a). In particular, as the  $\mu_{fix}$  becomes larger and embedment depth becomes deeper, the difference between  $\mu_{fix}$  and  $\mu_{max}$  becomes more remarkable. It means that earthquake responses considering only horizontal kinematic interaction are underestimated.

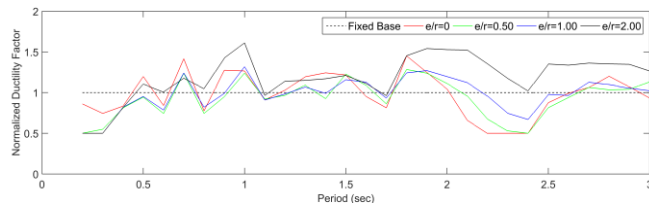
Next, the effect of RFIM on the buildings having long natural period is explained. When  $\mu_{fix}$  is small, the responses of buildings with natural periods more than 2 seconds except for the  $e/r = 2$  under considering RFIM are smaller than those of the fixed-base model. It is estimated that the input ground motion is reduced because the slender building with spread foundation on the soft ground is assumed and the rocking spring of the soil is relatively small and the natural period of the coupled system becomes long. However, if the embedment is deep ( $e/r = 2.0$ ) considering RFIM, it is seen that the response is increasing because of the small rocking stiffness. In addition, when  $\mu_{fix}$  is large,  $\mu_{max}$  values are larger than those of the  $\mu_{fix}$  values in some case of the natural period of buildings, even if the embedment is shallow.

Finally, importance of RFIM on the nonlinear response of buildings is evaluated generally. It is notable that the maximum ductility factor of the  $e/r = 2.0$  in Fig. 8 (a) are 1.5 times larger than that both of the fixed base model and (c) by means of the RFIM. Therefore, it can be said that unreasonable design is obtained for such conditions by neglecting KI or SSI. It suggests the possibility that the rocking input motion is a major impact in the near to the ultimate state situation of the building. However these results only valid for mat foundations, for pile foundations different study should be applied.

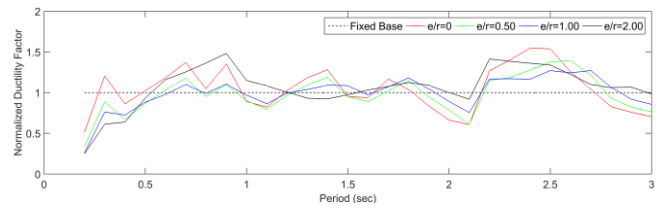
Fluctuation of ductility factors with changing natural frequency values is seen in these figures. Since, it is noticed that the global tendency of results may depend on the relationship between the spectral characteristics of the input ground motion and the equivalent natural period of the superstructure under the plastic deformation in this study.

On the other hand, if the shear wave velocity of the surface layers is as large as  $V_s = 200\text{m/s}$ , as shown in Fig.8(d-f), the variation due to the difference in the embedment depth is less in any natural period, and that it is found the response exhibits almost the same response as the fixed base model in the case of (d) and (f).

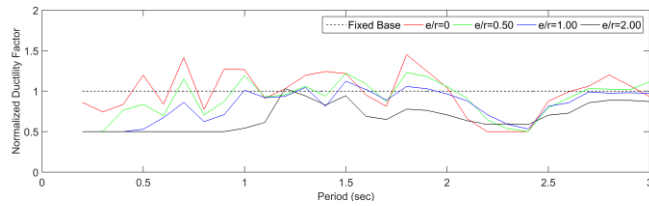
Maximum response ductility factor ratio of (a): with RFIM to (c): without KI is compared with each  $\mu_{fix}$  in Fig.9 where x-axis is same as Figs.7 and 8. When the ratio is larger than 1, it means that the response ductility factor is increased by taking into account RFIM. From this figure, it is observed that the response is underestimated in the case of the deep embedment foundation in 0.5 seconds or more of the building natural period if RFIM is neglected.



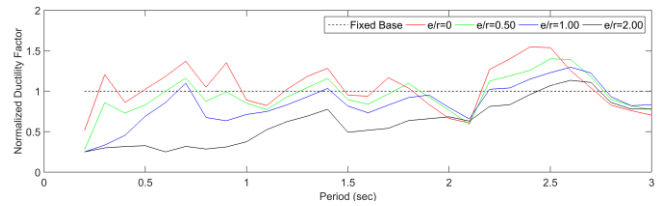
(a) With RFIM ( $V_s=100\text{m/s}$ ,  $\mu_{fix}=2$ )



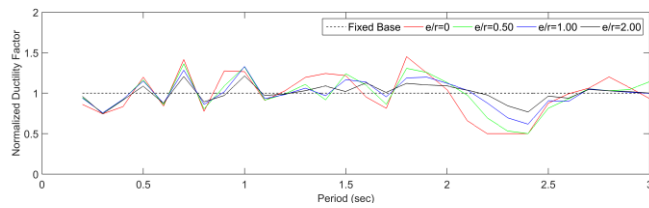
(d) With RFIM ( $V_s=100\text{m/s}$ ,  $\mu_{fix}=4$ )



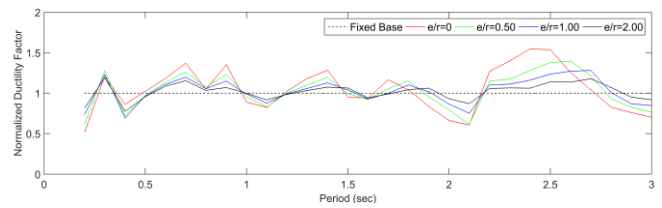
(b) Without RFIM ( $V_s=100\text{m/s}$ ,  $\mu_{fix}=2$ )



(e) Without RFIM ( $V_s=100\text{m/s}$ ,  $\mu_{fix}=4$ )

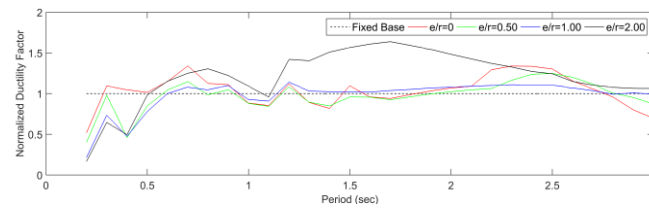


(c) Without KI ( $V_s=100\text{m/s}$ ,  $\mu_{fix}=2$ )

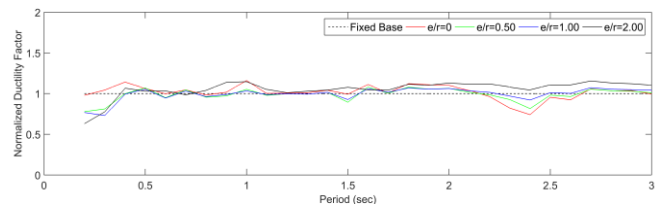


(f) Without KI ( $V_s=100\text{m/s}$ ,  $\mu_{fix}=4$ )

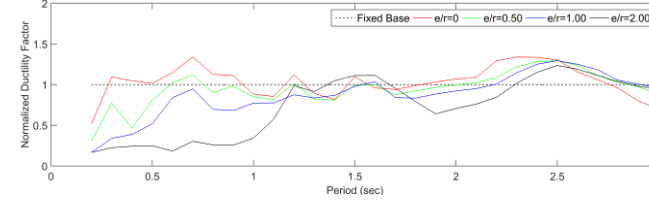
Fig. 7 – Ductility factors for Kobe Earthquake TAK000 component at Takatori Station with and without RFIM, and without KI ( $h=0.05$ ,  $r=10\text{m}$ ,  $\rho=1.8\text{t/m}^3$ ,  $\nu=0.42$ ,  $m=N*100\text{t}$ ,  $m_f/m=0.82$ )



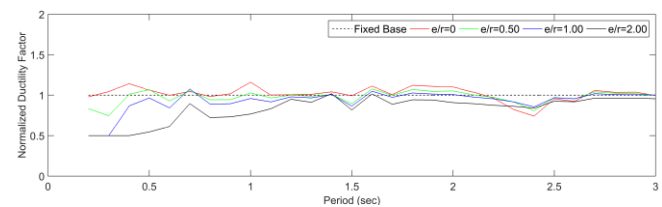
(a) With RFIM ( $V_s=100\text{m/s}$ ,  $\mu_{fix}=6$ )



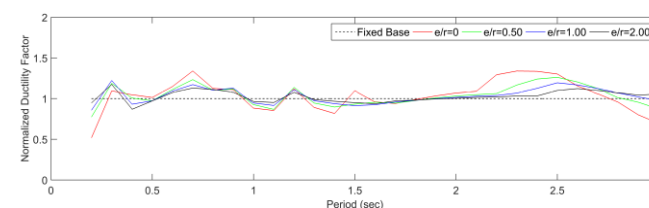
(d) With RFIM ( $V_s=200\text{m/s}$ ,  $\mu_{fix}=2$ )



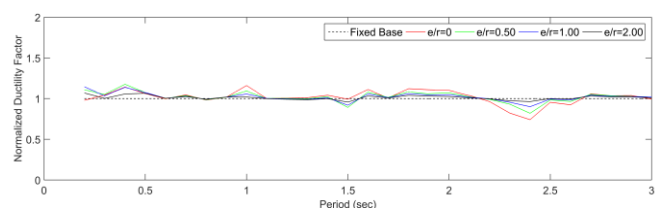
(b) Without RFIM ( $V_s=100\text{m/s}$ ,  $\mu_{fix}=6$ )



(e) Without RFIM ( $V_s=200\text{m/s}$ ,  $\mu_{fix}=2$ )



(c) Without KI ( $V_s=100\text{m/s}$ ,  $\mu_{fix}=6$ )



(f) Without KI ( $V_s=200\text{m/s}$ ,  $\mu_{fix}=2$ )

Fig. 8 – Ductility factors for Kobe Earthquake TAK000 component at Takatori Station with and without RFIM, and without KI ( $h=0.05$ ,  $r=10\text{m}$ ,  $\rho=1.8\text{t/m}^3$ ,  $\nu=0.42$ ,  $m=N*100\text{t}$ ,  $m_f/m=0.82$ )

### 4.2 Analysis results for Tohoku Earthquake Record

The results of  $V_s = 100\text{m/s}$  and  $\mu_{fix} = 6$  are shown in Fig.10. In this case, the observation records at K-NET Furukawa (MYG006) of the main shock (EW component) in the 2011 Tohoku region Pacific Ocean Earthquake is applied as an input ground motion. It is found that  $\mu_{max}$  fluctuates according to the spectral characteristic of the input ground motion in the long period domain. In Fig.11, maximum ductility factor ratio of (a): with RFIM to (c): without KI is compared to the case of  $\mu_{fix} = 6$ . The same tendency as that of the Kobe Earthquake is shown. From these results, it is concluded that inelastic building responses are not dependent strongly on duration of input ground motions in this study.

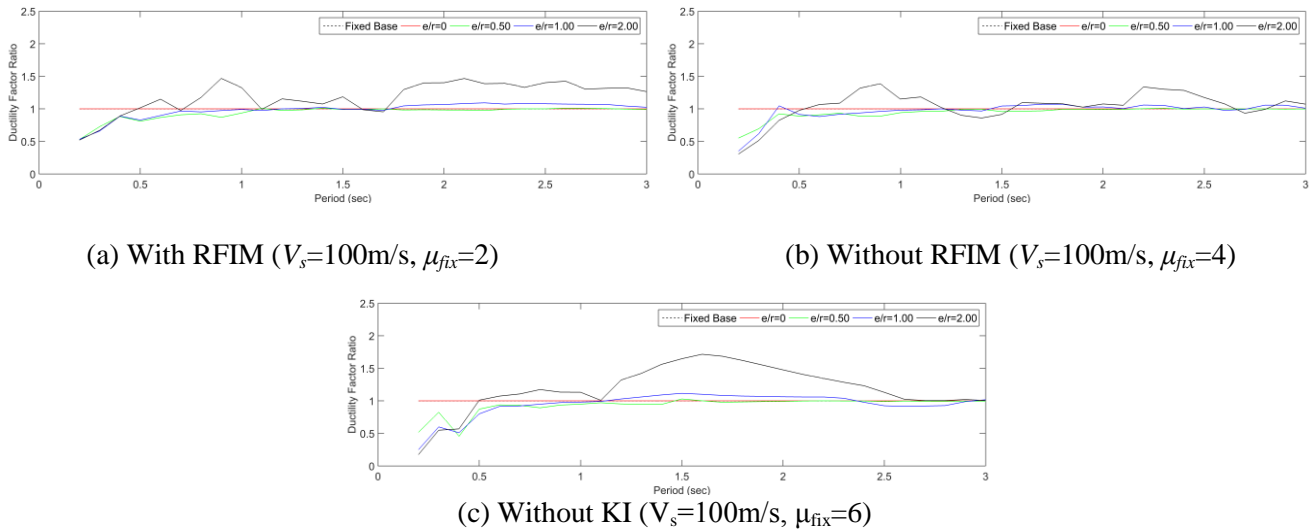


Fig. 9 – Ductility factor Ratios for Kobe Earthquake TAK000 component at Takatori Station with RFIM to without KI ( $h=0.05$ ,  $r=10\text{m}$ ,  $\rho=1.8\text{t/m}^3$ ,  $\nu=0.42$ ,  $m=N^*100\text{t}$ ,  $m_f/m=0.82$ )

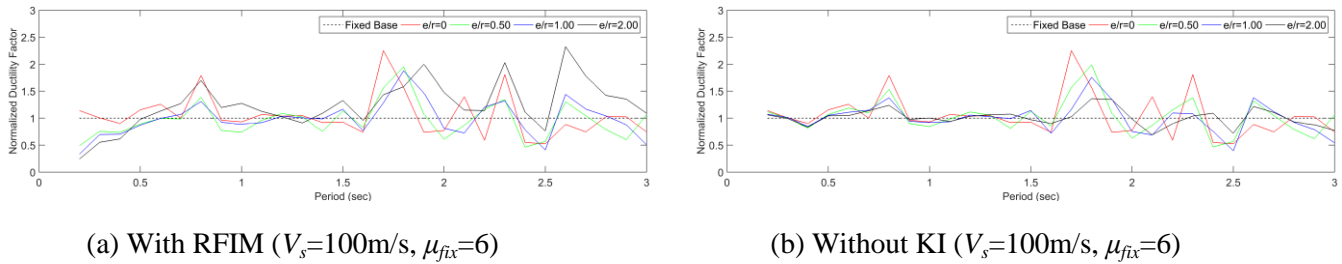


Fig. 10 – Ductility factors for Tohoku Earthquake EW component at MYG006 with RFIM, and without KI ( $h=0.05$ ,  $r=10\text{m}$ ,  $\rho=1.8\text{t/m}^3$ ,  $\nu=0.42$ ,  $m=N^*100\text{t}$ ,  $m_f/m=0.82$ )

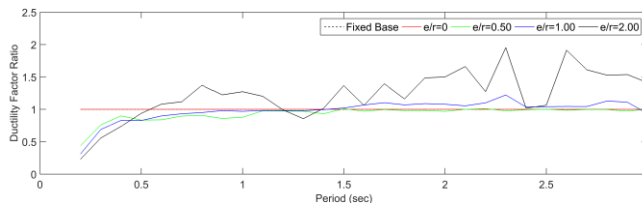


Fig. 11 – Ductility factor Ratios for Tohoku Earthquake EW component at MYG006 with RFIM to without KI ( $h=0.05$ ,  $r=10\text{m}$ ,  $\rho=1.8\text{t/m}^3$ ,  $V_s=100\text{m/s}$ ,  $\nu=0.42$ ,  $m=N^*100\text{t}$ ,  $m_f/m=0.82$ ,  $\mu_{fix}=6$ )



## 5. Conclusions

In this study a new LPM is constructed depends on the impedances of embedded foundations having different embedment depth placed on the elastic half-space for the  $\nu$  value equals to 0.42 and  $V_s$  value equals to 100 and 200 m/s to represent the soft soil conditions. Then nonlinear response analyses are carried out for SDOF elastoplastic structures, having fixed ductility capacity values as 2, 4, 6, and predominant periods from 0.2 to 3 seconds, and the improved LPM model under active fault and subduction zone earthquake records considering with and without RFIM to understand the effects of RFIM on the ductility demands of superstructures. Earthquake records both of Takatori Station record in the 1995 Hyogoken-Nanbu Earthquake (Kobe Earthquake) and the 2011 off the Pacific Coast of Tohoku Earthquake (Tohoku Earthquake) EW component of MYG006 Station are used for these analyses. The results of analyses are shown as follows;

- a. By increasing ductility factor values, the effect of RFIM becomes more severe, especially for high-rise buildings having embedment ratios bigger than 1. The reason of this phenomenon is explained that the equivalent elastic stiffness of superstructure becomes softer for increasing values of ductility capacity, therefore inertial interaction becomes less important and the additional force coming from the rocking motion becomes more important in the response of superstructure.
- b. For  $V_s=200$  m/s, the effect of RFIM is more stricted than  $V_s=100$ m/s, because the amplitude of RFIM decreases.
- c. RFIM should be considered for the collapse limiting design especially for the high rise building having embedment ratios bigger than 1 in this case. Even the design neglecting the KI effect, underestimates the effect of earthquakes in some critical situations.

However, it should be noted that these results are obtained for restricted parameters. For more reliable results, considered parameters in the analyses should be increased.

## 6. Acknowledgements

In this study, the program coded by Doctor Xuezhang Wen is used. The authors gratefully acknowledge contribution of him.

## 7. References

- [1] Ogut OC, Mori M, Fukuwa N (2016): Effect of rocking foundation input motion on the inelastic behavior of structures. *J. Struct. Constr. Eng. AIJ*, Vol. 81, No. 721, .447-457.
- [2] Jennings PC, Bielak J (1973): Dynamics of buildings–soil interaction. *Bulletin of Seismological Society of America*, 63(1), .9–48.
- [3] Veletsos AS, Meek JW (1974): Dynamic behavior of building–foundation system. *Earthquake Engineering and Structural Dynamics*, 3(2), 121–138.
- [4] Veletsos AS, Nair VVD (1975): Seismic interaction of structures on hysteretic foundations. *Journal of the Structural Division (ASCE)*, 101(1), 109–129.
- [5] Veletsos AS (1977): Dynamics of structure–foundation systems. *In Structural and Geotechnical Mechanics*, Hall WJ (ed.), A Volume Honoring N.M. Newmark. Prentice-Hall: Englewood Cliffs, NJ, 333–361.
- [6] Bielak J (1975): Dynamic behavior of structures with embedded foundations. *Earthquake Engineering and Structural Dynamics*, 3(3), 259–274.
- [7] Avilés J, Pérez-Rocha LE (1996): Evaluation of interaction effects on the system period and the system damping due to foundation embedment and layer depth. *Soil Dynamics and Earthquake Engineering*, 15(1), 11–27.
- [8] Applied Technology Council. Tentative provisions for the development of seismic regulations for buildings. ATC-3-06, California, 1978.



- [9] Building Seismic Safety Council (BSSC). NEHRP Recommended Provisions for Seismic Regulations for New Buildings and Other Structures. Federal Emergency Management Agency, Washington, DC, 2000.
- [10] Building Seismic Safety Council (BSSC). NEHRP Recommended Provisions for Seismic Regulations for New Buildings and Other Structures. Federal Emergency Management Agency, Washington, DC, 2004.
- [11] FEMA 440. Improvement of nonlinear static seismic analysis procedures. Report No. FEMA 440, Federal Emergency Management Agency, prepared by Applied Technology Council, 2005.
- [12] Building Seismic Safety Council (BSSC). NEHRP Recommended Provisions for Seismic Regulations for New Buildings and Other Structures. Federal Emergency Management Agency, Washington, DC, 2015.
- [13] Structure related technical standard manual for buildings (2007 year edition) (in Japanese), Structure related technical standard manual for buildings edit committee, 2008.6. (In Japanese)
- [14] Luco JE, Wong HL, Trifunac MD (1975): A note on the dynamic response of rigid embedded foundations. *Earthquake Engineering and Structural Dynamics*, 4(2), 119–127.
- [15] Morray JP (1975): Kinematic interaction problem of embedded circular foundations. M.Sc. Thesis, Department of Civil Engineering, Massachusetts Institute of Technology.
- [16] Veletsos AS, Verbic B (1973): Dynamics of elastic and yielding structure–foundation systems. *Proceedings of Fifth World Conference on Earthquake Engineering*, Rome, Italy, 2610–2613.
- [17] Bielak J (1978): Dynamic response of non-linear building–foundation systems. *Earthquake Engineering and Structural Dynamics*, 6(1), pp.17–30.
- [18] Lin YY, Miranda E (2008): Kinematic soil–structure interaction effects on maximum inelastic displacement demands of SDOF systems. *Bulletin of Earthquake Engineering*, 6(2), 241–259.
- [19] Jarenpasert, Sittipong, Enrique Bazan-Zurita, Bielak J.: Seismic soil-structure interaction response of inelastic structures. *Soil Dynamics and Earthquake Engineering*, 47, pp.132-143, 2013.
- [20] Ptilakis, D, Makris, N (2010): A study on the effects of the foundation compliance on the response of yielding structures using dimensional analysis. *Bulletin of Earthquake Engineering*, 8(6), 1497-1514.
- [21] Karatzetou A, Ptilakis D (2013): Performance-based seismic demand soil-foundation-structure systems. *4th ECCOMAS Thematic Conference on Computational Methods in Structural Dynamics and Earthquake Engineering*.
- [22] Mahsuli M, Ghannad MA (2009): The effect of foundation embedment on inelastic response of structures. *Earthquake Engineering & Structural Dynamics*, 38(4), 423-437.
- [23] Wolf JP (1994): Foundation vibration analysis using simple physical models. Pearson Education.
- [24] Meek JW, Wolf JP (1994): Cone models for embedded foundation. *Journal of geotechnical engineering*, 120.1, 60-80.
- [25] Wolf JP, Deeks AJ (2004): Foundation vibration analysis: A strength of materials approach. Butterworth-Heinemann.
- [26] Wen, H (2006): An Analytical Study on Effects of Foundation Type, Foundation Shape and Adjacent Building on Dynamic Soil Structure Interaction. Diss. Nagoya University. (In Japanese)